Numerical Study on Overtopping Performance of Multi-stage Overtopping Wave Energy Converter

Guoliang Zhang, Xiaoxia Zhang, Chuanli Xu, Xiaochen Dong, and Zhen Liu*

Abstract— **The characteristics of wave conditions with large tidal ranges and small wave heights in China's coastal waters limit the operation time of traditional single-stage overtopping devices, whereas the multi-stage overtopping wave energy converters can increase the overall operation time of the device by distributing the upper and lower reservoirs. To study the overtopping performance of the multi-stage overtopping wave energy converter under real sea conditions, a two-dimensional numerical model of the device is developed and verified by physical model tests. The effects of the lower reservoir opening width, slope angle combination, and slope inundation length on the overtopping performance are investigated under regular wave conditions. We found that a smaller opening width and two 30° slope angles improve the overtopping performance of the device. Further, based on the full-scale prototype device, the database of overtopping in a complete tidal cycle (12h) were constructed under real sea conditions to provide the basic data for the Wave-to-wire model of power generation simulation.**

Keywords—**Overtopping wave energy converter; Structural parameters; Overtopping database; Numerical simulation.**

Sponsor and financial support acknowledgement: For example, "This work was supported in part by the National Natural Science Foundation of China under grant U1906228, Fundamental Research Funds for the Central Universities under grant 202313031, Qingdao Postdoctoral Program Grant under grant QDBSH20220201015".

Guoliang, Z is with Shandong Provincial Key Laboratory of Ocean Engineering, Ocean University of China, 238 Songling Road, Qingdao, China (e-mail: zhanggl1994@163.com)

Xiaoxia, Z is with Shandong Provincial Key Laboratory of Ocean Engineering, Ocean University of China, 238 Songling Road, Qingdao, China (e-mail: zhangxiaoxia@stu.ouc.edu.cn)

Chuanli, X is with Shandong Provincial Key Laboratory of Ocean Engineering, Ocean University of China, 238 Songling Road, Qingdao, China (e-mail: xuchuanli@stu.ouc.edu.cn)

Xiaochen, D is with Shandong Provincial Key Laboratory of Ocean Engineering, Ocean University of China, 238 Songling Road, Qingdao, China (e-mail: dongxiaochen@ouc.edu.cn)

Liu, Z is with Shandong Provincial Key Laboratory of Ocean Engineering, Ocean University of China, 238 Songling Road, Qingdao, China (e-mail: liuzhen@ouc.edu.cn)

Digital Object Identifier: https://doi.org/10.36688/ewtec-2023-584

I. INTRODUCTION

Overtopping wave energy converters can be combined with breakwater and shore protection projects while exploiting wave energy, and changing the passive energy dissipation of coastal projects into active energy absorption [1] [2] [3]. However, this type of device has poor adaptability to tidal level changes, which will seriously affect the working head that is extremely sensitive to water level changes, resulting in a short effective working time of the device and low overall efficiency and hourly average power generation output level. The multi-stage overtopping wave energy converter designed in this study is designed to adapt to the problem of large tidal differences in the northern waters of China, and the device has two levels of reservoirs, which can work separately at high and low water levels to increase the effective working time of the device and improve the overall power output level [4].

Among the studies on stationary overtopping wave energy converters, the world's first stationary overtopping wave energy converter, TAP CHAN, was built in Norway in 1985 with an installed capacity of 350 kW [5] [6]. For single-stage reservoir devices, researchers focused on the effect of geometry on the overtopping discharges [7] [8] [9] [10]. Kofoed studied the effect of slope angle, slope shape, and crest freeboard height on overtopping performance through model tests and obtained a range of slope angles and crest freeboard heights that are more suitable for the devices [7]. Liu et al. compared the effects of different slope ratios on overtopping performance and concluded that the smaller the slope ratio, the less the amount of overtopping discharges [8]. On this basis, the effects of different slope shapes were further compared, and it was concluded that the convex slope has the best overtopping performance, but it is difficult to build in practice, and the flat slope shape is generally used [9]. Victor et al. studied the effect of structural parameters of the device and explored that the optimal range of the slope angle α of the device is $0 \leqq \cot\alpha \leqq 6$, and the optimal range of relative crest freeboard height is $R_c/H_{m0} < 1.5$ [10].

To enhance the overtopping performance by collecting more water under large wave height conditions, Kofoed et al. investigated Seawave Slot-cone Generator (SSG) using a multi-stage reservoir and summarized the

structural design, reliability, and overall performance of the SSG through experimental measurements and numerical simulations [11] [12] [13] [14] [15]. It was found that the hydraulic efficiency of the device can be substantially improved by using a five-stage reservoir design compared to a single-stage reservoir [11]. Meanwhile, the overtopping performance is optimal at a slope angle of 19°, but the design of 35° can effectively reduce the energy loss due to wave breaking [15]. Based on the design of SSG, Overtopping BReakwater for Energy Conversion (OBREC), which is combined with conventional breakwaters, was proposed, and experimental studies of overtopping performance and structural loading were carried out [16] [17] [18]. The simulation of the overtopping wave phenomenon was performed for OBREC installations using Flow 3D and the accuracy of the model was verified [19]. Currently, the prototype OBREC device was constructed and put into operation in the Port of Naples [20].

In the process of developing and utilizing ocean energy, the prediction of wave power generation can help to make more scientific and reliable decisions on the sea trial of the device, and further improve the performance of the device while avoiding the waste of resources. Based on optimizing the structure of the multi-stage overtopping wave energy converter, numerical simulation is used to estimate the overtopping discharges, to build a database of the basic overtopping discharges of the prototype device under real sea conditions, to provide a basis for the prediction of the final device power generation, and to provide a new set of ideas for the performance study of this type of wave-energy generation device.

II. NUMERICAL MODEL

A. Model Design

The model design of the multi-stage overtopping wave energy converter is shown in Figure 1. Referring to previous research [21], the slopes of the upper and lower slopes are defined as β and α. The slope heights of the upper and lower slopes are defined as R_U and R_L,

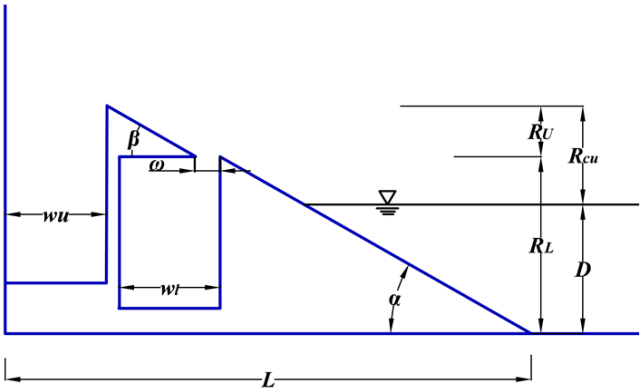

Fig. 1. Model of a multi-stage overtopping wave energy converter.

respectively, with fixed slope heights R_U = 0.1m and R_L = 0.4m. The crest freeboard height of the upper slope is denoted by R_{cu}. The widths of the lower reservoir openings are denoted by ω. These widths are measured horizontally and the width of the lower reservoir(LR) and the upper reservoir(UR) are defined as wl = wu =0.2m, L denotes the total length of the installation, and D is the water depth.

B. Numerical modeling and validation

The two-dimensional numerical wave tank uses a combination of quadrilateral and triangular meshes, with a triangular mesh at the device and a quadrilateral mesh at the tank section. The grid is refined at the key structure of the device and the free surface. The height of the grid at the free surface is 1/20 of the wave height H, and the width of the grid in the wave run direction is 1/50 of a wavelength λ. The wall boundary is used at the left side of the device and the right side of the wave maker and the bottom surface, and the pressure outlet boundary condition is at the top of the tank, as shown in Figure 2.

The calculations use the continuity equation and the RANS (Reynolds-averaged Navier-Stokes) equation as the controlling equations for the fluid flow. The VOF (Volume of Fluid) model is used to track the free water surface, which is set to water and air by user-defined materials. The RNG k-ε turbulence model was used to close the control equations. All equations were solved using the finite volume method in the CFD software

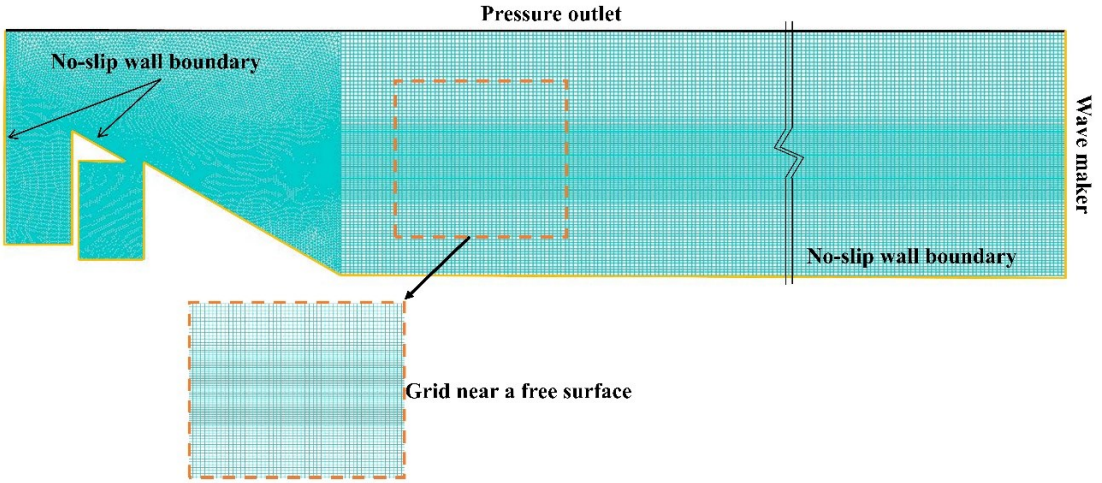

Fig. 2. Boundary conditions and mesh in the numerical wave tank.

ANSYS-Fluent® 16.0. The PISO(pressure implicit with splitting of operators) algorithm is used for pressure velocity coupling. The LSCB(Least Squares Cell-Based) method is used for gradient interpolation. The time-step is set up to be 1/200, and a total of 15 stable incident regular waves are monitored during the simulation.

To test the accuracy of the numerical wave tank calculations, some of the test conditions of [4] were selected for validation. The width and length of the wave tank used in experimental test are 0.6 m and 30.0 m respectively, and the depth is 1.0 m. A sponge zone with a length of 2.0 m is set up at the end of the tank, and the device is located 23.0 m away from the wavemaker. In the simulation process, because the overtopping water can not cross the device, the numerical flume does not set the sponge zone, the device is located at the end of the numerical tank, 23.0 m away from the wavemaker.

The test condition of D=30cm, wave height H=10 cm, period T=1.0s, α=β=30°, ω=5cm is selected. Snapshot comparisons of the overtopping process in a wave cycle between the numerical prediction and experimental test are shown in Figure 3. At t= T/4, the wave water starts to climb under the action of the slope to the lower reservoir. In the experimental test, wave breaking was observed at the opening, and although it was a difficult task to obtain details of wave breaking at the water tongue from the simulation results, the water surface profile at this point could be matched. At t=2T/4, the wave water climbs along the upper slope into the upper reservoir, at which point the numerical simulation results in a free water surface slightly higher than the test. At t=3T/4, the wave water falls back and enters the lower reservoir in large quantities. At t=T, the wave water falls back down to the lower slope.

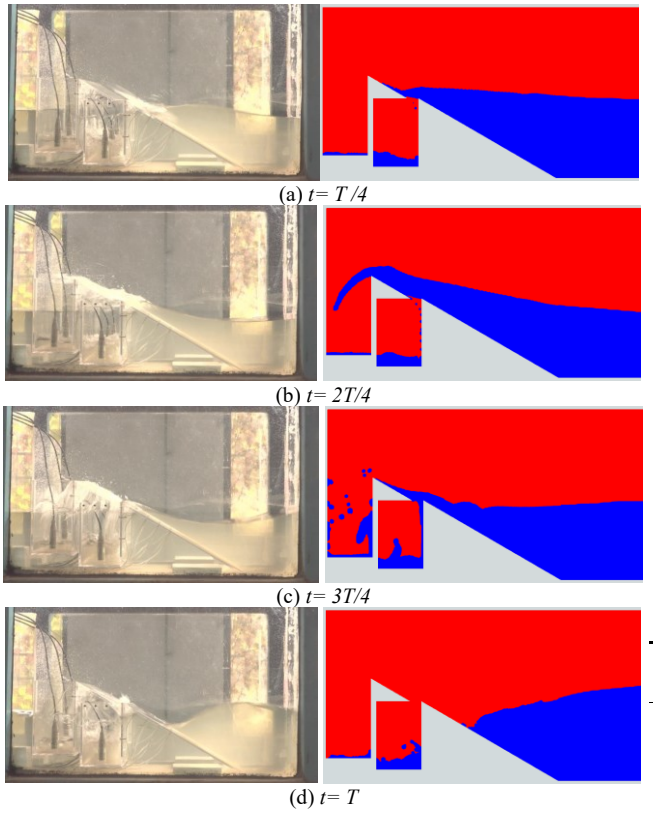

Fig. 3. Snapshot comparison of the overtopping process in a wave cycle between experimental and numerical results.

Overtopping discharges are the main performance index for evaluating the performance of the device. To eliminate the influence of wave height in the process of evaluating the operational performance of the equipment, the data are dimensionless.

The dimensionless overtopping discharges for the LR and UR are defined as Q_L and Q_U, which can be expressed as [22]:

$$\text{Q\_L} = \frac{q_L}{H\sqrt{gH}}, \text{Q\_U} = \frac{q_U}{H\sqrt{gH}} \quad (1)$$

Where: q_L and q_U are the time-averaged overtopping discharges per meter (m^3/m/s), respectively, H is the incident wave height, and g is the acceleration of gravity.

During the simulation, at least 15 waves were monitored for each case to obtain more accurate simulation results. The experimental results of [4] were selected for validation, where β = α = 30°, ω is 10 cm, water depth D is 40 cm, wave height H is 7.5 cm, periods T are 0.8 s, 1 s, 1.2 s, 1.4 s, and the relative wavelength is defined as r_L = λ/L. The comparison between the experimental results and the numerical simulation results for different incident periods is given in Figure 4. From the figure, it can be seen that the overtopping discharges data obtained from the experimental and numerical simulations show a basic consistent trend with the variation of the incident wave period, and the maximum error between the two is 5.1%

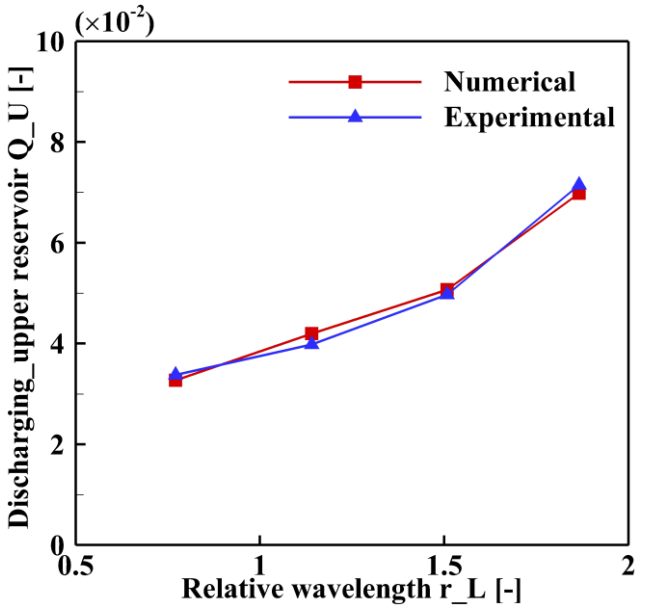

Fig. 4. Comparison of numerical and experimental dimensionless overtopping discharges (H=7.5cm).

III. RESULTS AND DISCUSSION

C. *Effects of structural parameters on the overtopping discharges of UR*

Under regular wave conditions, the effect of structural parameters (including LR opening width ω and upper

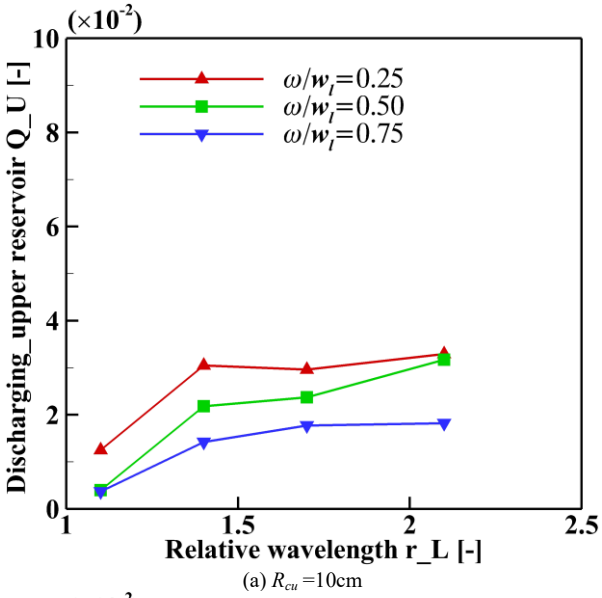

(a) R_{cu} =10cm

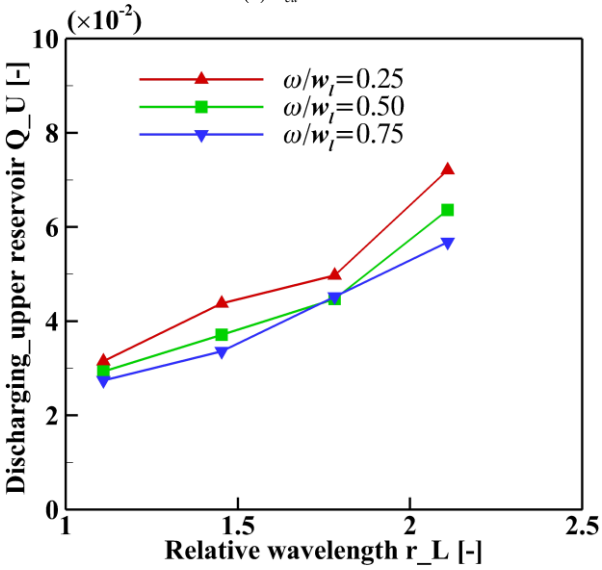

(b) R_{cu} =5cm

Fig. 5. Effects of the ω on the dimensionless overtopping discharges of UR (H = 9cm).

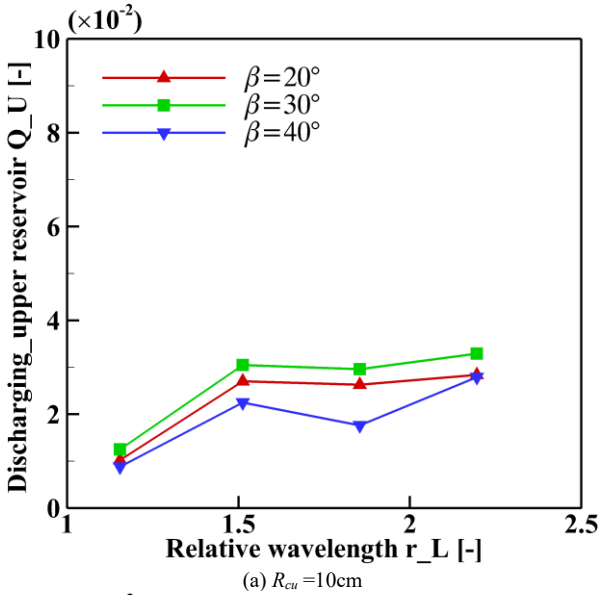

(a) R_{cu} =10cm

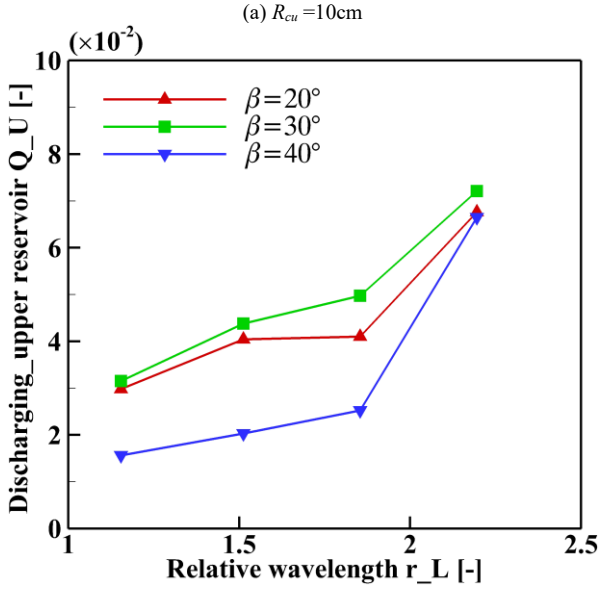

(b) R_{cu} =5cm

Fig. 6. Effects of the β on the dimensionless overtopping discharges of UR (H = 9cm).

slope angle β) on the overtopping discharges is studied. The test-run series for various values of ω and β are listed in Table 1. Different from the previous study[21], this paper selects the small period incident wave to be more in line with the actual wave conditions in the target sea area, and as a supplement to the original study, the period of the incident wave is set to be 1.0s, 1.25s, 1.5s, 1.75s.

To study the effect of LR opening width on the overtopping discharges of UR, the slope of the fixed upper and lower slopes α=β=30°, and Figure 5 shows the variation of the Q_U with three different ω under different incident wave conditions at R_{cu} of 10 cm and 5 cm, respectively. ω/w_l is the relative opening width of the LR.

When the R_{cu} =10 cm, the Q_U gradually decreases as the opening increases. For different r_L, the mean value of the Q_U with a 5 cm opening is 23% and 49% higher than those with 10 cm and 15 cm openings, respectively. When the R_{cu} = 5 cm, the lower reservoir is in a completely submerged state, and the maximum values of the Q_U of the three openings are 7.21, 6.36, and 5.68 for different r_L, respectively, and the mean values of the Q_U with 5 cm was 11.4% and 17.3% higher than those with 10 cm and 15 cm opening, respectively. Under different wave conditions, UR showed better overtopping performance for ω=5cm. The reason for this is that the overtopping water will break up after passing through the LR opening area, resulting in a large loss of kinetic energy. The larger the opening, the more pronounced the wave breakage, so less overtopping water continues to climb up the upper slope, and thus less water enters the UR.

To study the effect of the upper slope angle β on the overtopping performance of the UR, fixed ω=5cm, α=30°. Figure 6 shows the variation of the Q_U with three different β under different incident wave conditions at R_{cu} of 10 cm and 5 cm, respectively.

When the R_{cu} = 10 cm, the UR with β = 30° exhibits the optimal overtopping performance at different values *of* r_L for the incident wave height of 9 cm. When the R_{cu} was reduced to 5 cm, the LR was in the submerged state and the Q_U with a 5 cm opening was 11.4% and 17.3%

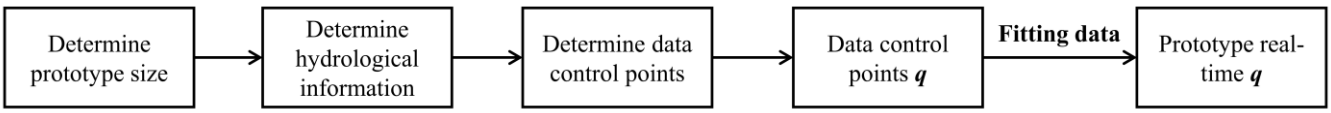

Fig.7. Real-time overtopping discharges simulation flow of the prototype device.

higher than those with 10 cm and 15 cm openings, respectively. As the water depth increases, the steep slope makes it difficult for the overtopping water to climb into the reservoir. In addition, a gentle slope increases the length of the overtopping water climbing path, which also leads to energy loss during wave propagation. Therefore, the β = 30° exhibits better overtopping performance under the effect of slope lift of the LR.

It was found that the overtopping device showed better performance under different incident wave working conditions with α=β=30°, ω=5cm, which is consistent with the results of previous studies[21].

D. Prototype device overtopping discharges simulation

To simulate the overtopping discharges of the device prototype at different tide levels under actual sea conditions, to obtain the basic data of the overtopping discharges of the device prototype at different moments in a tide cycle, and to provide the basic data for the estimation of the annual power generation of the device prototype under typical wave conditions. In this paper, the measured hydrographic information of the target sea area is used to determine the dimensions of the prototype device and the average tidal surface, and the irregular wave simulation is carried out under different tidal conditions to obtain the wave-crossing volume of the prototype device, and the specific simulation process is shown in Figure 7.

(1) Determine prototype device sizing. Based on the optimized model of the device, the size of the prototype was enlarged according to the scale of 1:16. The length of both the upper and lower reservoirs of the prototype is 30m, the width of the reservoirs is 3.2m, the depth of the upper and lower reservoirs is 2.4m and 2.0m respectively, and the lower reservoirs opening is 0.8m.

(2) Determine the hydrographic information of the sea area. The prototype of the device is to be placed in the northern part of the Yellow Sea. Based on one year of continuous statistical data from deployed ocean observation buoys, the annual average effective wave height H_s is 0.6m, and the effective period T_s is 4.0s.

The monthly mean tidal range of the sea area where the prototype of the device is proposed to be placed is about 3.0 m in a year, and the statistical value of the monthly tidal range is shown in Figure 8. The sea area is in line with the characteristics of the tidal level change of the regular half-day tide, and to accurately identify the corresponding drywall heights at different tidal levels, the tidal level change in this sea area is assumed to be a regular sinusoidal change curve, with the equation y = 1.5sin (2πt/12), and the change of one tidal cycle is shown in Figure. 9.

(3) In a complete tidal cycle, determine the data control points. According to the tidal difference of 3 meters in the sea, the elevation of the LR is +0.2 m, and the UR is +1.8 m, as shown in Figure 10. Based on the tide level change in one tide cycle of the sea, a total of 14 data control points were selected for hourly tide level points and 2

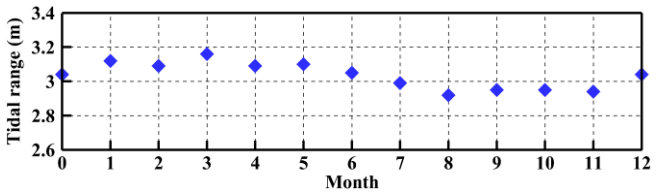

Fig. 8. Monthly tidal variation in the sea area.

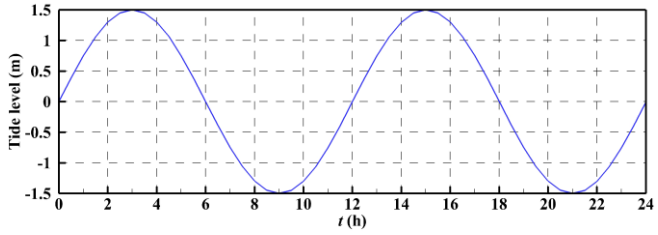

Fig. 9. Tide level course line in one day.

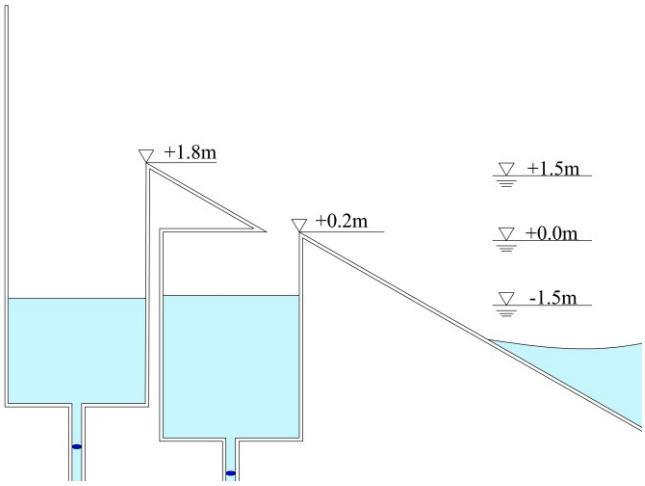

Fig. 10. Elevation diagram of prototype device.

TABLE II
DATA CONTROL POINT ELEVATION

Hours (h)	Elevations (m)
0	1.8
0.26	1.6
1	1.05
2	0.5
3	0.3
4	0.5
5	1.05
5.26	1.6
6	1.8
7	2.55
8	3.1
9	3.2
10	2.55
11	1.8

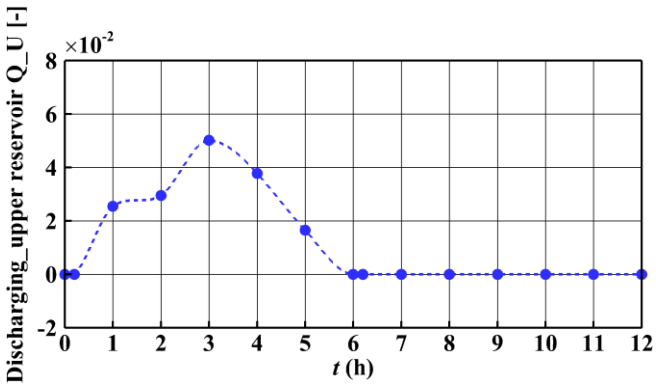

(a) UR

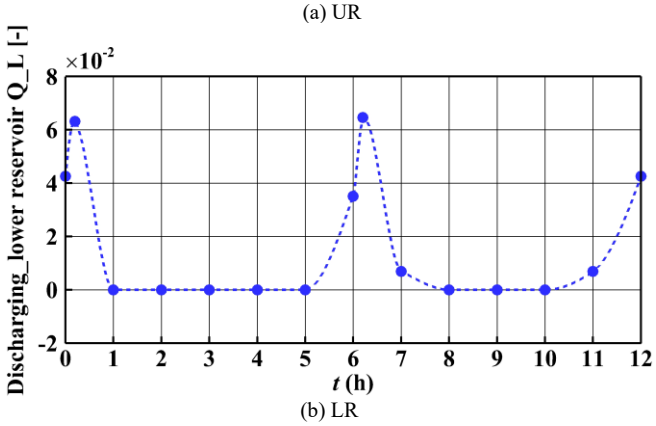

(b) LR

Fig. 11. Real-time overtopping discharges in UR and LR.

special points of tide level change (elevation +0.2m) respectively. The data of the slope top elevation corresponding to the data control points are shown in Table 2.

(4) Incident wave database generation and data control point overtopping discharges simulation. According to the H_s and T_s of sea area, we generate irregular wave columns (the number of waves is more than 100) for different times, and substituted into the determined 14 data control point for simulation, and the overtopping discharges at different tide levels are calculated.

(5) Fits data control points to generate real-hours overtopping discharges data for a complete tidal cycle. Based on the overtopping discharges corresponding to 14 data control points, the base data of overtopping discharges under different tidal conditions in a complete tidal cycle are fitted. Figure 11 shows the real-hours data of overtopping discharges in the UR and LR from 0 to 12 hours.

It can be seen from Fig. 11, the overtopping discharges of the UR are mainly concentrated 0-6 times, and the overtopping moment of the LR mainly occurs 0-1 time, 5-8 times, and 10-12 times. 1-5 times the LR is basically in the inundation state, whereas for 6-12 times, the UR fails to generate overtopping waves due to the large crest freeboard. The maximum Q_U was 0.053 near 3 time, and the maximum Q_L was 0.063 near 6 time.

IV. CONCLUSION

The multi-stage overtopping wave energy converter is a kind of power generation device which learns the design idea of SSG and adapts to the characteristics of large tidal differences in the Chinese sea.

1. The effect of the main structural parameters of the device (including LR opening width ω and upper slope angle β) on the overtopping discharges was studied by numerical simulation under regular wave conditions with different crest freeboard heights and incident wave combinations. The calculation results show the best overtopping performance with an LR opening width of 5cm and the combination of upper and lower slope angles of 30° and 30°.

2. Based on the structure-optimized device model, the overtopping discharges of different times were simulated under irregular wave conditions based on the device elevation and the actual hydrographic conditions of the engineering sea, and the overtopping discharges database of the prototype device under actual sea conditions was established. The results show that the maximum overtopping discharges of upper and lower reservoirs are 0.053 and 0.063, respectively. Using the established database, the power generation of the device can be evaluated by formulating the working strategy of the reservoir.

REFERENCES

[1] V Ramos, G Giannini, T Calheiros-Cabral, P Rosa-Santos, F Taveira-Pinto. "An Integrated Approach to Assessing the Wave Potential for the Energy Supply of Ports: A Case Study," *J Mar Sci Eng*, vol. 10, 2022. Accessed on: January, 12, 2023, DOI: 10.3390/jmse10121989, [Online]

[2] T Calheiros-Cabral, D Clemente, P Rosa-Santos, F Taveira-Pinto, V Ramos, T Morais, H Cestaro. "Evaluation of the annual electricity production of a hybrid breakwater-integrated wave energy converter," *Energy*, vol. 213, 2020. Accessed on: February, 18, 2023, DOI: 10.1016/j.energy.2020.118845, [Online]

[3] D Vicinanza, E D Lauro, P Contestabile, C Gisonni, J L. Lara, I J. Losada. "Review of innovative harbor breakwaters for wave-energy conversion," *J Waterw Port Coast Ocean Eng*, vol 145, 2019. Accessed on: February, 18, 2023, DOI: 10.1061/(ASCE)WW.1943-5460.0000519, [Online]

[4] Z Liu, Z Han, H Shi, W Yang. "Experimental study on multi-level overtopping wave energy convertor under regular wave conditions," *Int J Nav Arch Ocean*, vol 10, no 3, pp. 651-659, 2018. Accessed on: June, 11, 2021, DOI: 10.1016/j.ijnaoe.2017.10.004, [Online]

[5] A F O Falcão. "Wave energy utilization: A review of the technologies," *Renew Sustain Energy Rev*, vol 14, no 3, pp. 899-918, 2010. Accessed on: September, 08, 2021, DOI: 10.1016/j.rser.2009.11.003, [Online]

[6] Y Zhang, Y Zhao, W Sun, J Li. "Ocean wave energy converters: technical principle, device realization, and performance evaluation," *Renew Sustain Energy Rev*, vol 141, 2021. Accessed on: January, 25, 2022, DOI: 10.1016/j.rser.2021.110764, [Online]

[7] J P Kofoed, "Wave overtopping of Marine Structures: utilization of wave energy," Ph.D. Department of Civil Engineering Aalborg University, Aalborg, Denmark, 2002.

[8] Z Liu, B S Hyun, J Jin. "2D computational analysis of overtopping wave energy convertor," *J Korean Soc Ocean E*, vol 23, no 6, pp. 1-6, 2009. Accessed on: December, 06, 2021, [Online]

[9] Z Liu, B S Hyun, J Jin. "Computational analysis of parabolic overtopping wave energy convertor," *J. Korean Soc. Mar. Environ. Saf*, vol 12, no 4, pp. 273-278, 2009. Accessed on: December, 08, 2021, [Online]

[10] L Victor, P Troch. "Wave overtopping at smooth impermeable steep slopes with low crest freeboards," *J Waterw Port Coast Ocean Eng*, vol 138, no 5, pp. 372-385, 2012. Accessed on: April, 06, 2023, DOI: 10.1061/(ASCE)WW.1943-5460.0000141, [Online]

[11] J P Kofoed, "Model testing of the wave energy converter Seawave Slot-Cone Generator," in *Hydraulics and Coastal Engineering*, Department of Civil Engineering, Aalborg University, 2005, pp. 31-33. [Online] Available: https://vbn.aau.dk/en/publications/model-testing-of-the-wave-energy-converter-seawave-slot-cone-gene

[12] D Vicinanza, P Frigaard. "Wave pressure acting on a seawave slot-cone generator," *Coast Eng*, vol 55, no 6, pp. 553-568, 2008. Accessed on: June, 25, 2021, DOI: 10.1016/j.coastaleng.2008.02.011, [Online]

[13] L Margheritini, D Vicinanza, P Frigaard. "SSG wave energy converter: Design, reliability and hydraulic performance of an innovative overtopping device," *Renew Energ*, vol 34, no 5, pp. 1371-1380, 2009. Accessed on: June, 20, 2021, DOI: 10.1016/j.renene.2008.09.009, [Online]

[14] D Vicinanza, L Margheritini, J P Kofoed, M Buccino. "The SSG wave energy converter: Performance, status and recent developments," *Energies*, vol 5, no 2, pp. 193-226, 2012. Accessed on: August, 03, 2021, DOI: 10.3390/en5020193, [Online]

[15] J P Kofoed, T Hald, P B Frigaard. "Experimental study of a multi level overtopping wave power device," in *Proceedings of the 10th Congress of International Maritime Association of the Mediterranean*, Crete, Greece 2002.

[16] D Vicinanza, J H Nørgaard, P Contestabile, T L Andersenet. "Wave loadings acting on overtopping breakwater for energy conversion," *J Coast Res*, vol 65, pp. 1669-1674, 2013. Accessed on: August, 18, 2021, DOI: 10.2112/SI65-282.1, [Online]

[17] D Vicinanza, P Contestabile, J Q H Nørgaard, T L Andersenet. "Innovative rubble mound breakwaters for overtopping wave energy conversion," *Coast Eng*, vol 88, pp. 154-170, 2014. Accessed on: October, 11, 2022, DOI: 10.1016/j.coastaleng.2014.02.004, [Online]

[18] P Contestabile, C Iuppa, E D Lauro, L Cavallaro, T L Andersenet, D Vicinanza. "Wave loadings acting on innovative rubble mound breakwater for overtopping wave energy conversion," *Coast Eng*, vol 122, pp. 60-74, 2017. Accessed on: February, 17, 2023, DOI: 10.1016/j.coastaleng.2017.02.001, [Online]

[19] C Iuppa, P Contestabile, L Cavallaro, E Foti, D Vicinanza. "Hydraulic performance of an innovative breakwater for overtopping wave energy conversion," *Sustainability*, vol 8, no 12, 2016. Accessed on: February, 21, 2023, DOI: 10.3390/su8121226, [Online]

[20] P Contestabile, G Crispino, E D Lauro, V Ferrante, C Gisonni, D Vicinanza. "Overtopping breakwater for wave energy conversion: review of state of art, recent advancements and what lies ahead," *Renew Energ*, vol 147, pp. 705-718, 2020. Accessed on: December, 16, 2022, DOI: 10.1016/j.renene.2019.08.115, [Online]

[21] Z Liu, Z Han, H Shi. "Numerical study on overtopping performance of a multi-level breakwater for wave energy conversion," *Ocean Eng*, vol 150, pp 94-101, 2017, DOI: 10.1016/j.oceaneng.2017.12.058, [Online]

[22] N Kobayashi, A Wurjanto. "Wave overtopping on coastal structures," *J Waterw Port Coast Ocean Eng*, vol 115, no 2, pp. 235-251, 1989. Accessed on: November, 22, 2022, DOI: 10.1061/(ASCE)0733-950X(1989)115:2(235), [Online]